Microfluid Nanofluid (2011) 10:627–635
DOI 10.1007/s10404-010-0696-y

L-Malic acid production within a microreactor with surface immobilised fumarase

Gorazd Stojkovič · Igor Plazl · Polona Žnidaršič-Plazl

Received: 9 July 2010 / Accepted: 5 August 2010 / Published online: 10 October 2010

Abstract In recent years, microreactors have evolved from a technical novelty to a useful tool in many scientific laboratories. On the other hand, their implementation in industry proceeds with a slower pace. In this work, we present a microreactor system for continuous L-malic acid production that demonstrates potentials of microfluidic systems for production of this widely used organic acid. APTES and glutaraldehyde were used to covalently immobilise fumarase on glass microreactor walls in order to allow product–catalyst separation. The system was tested at different substrate concentrations and flow rates and conversion up to 80% could be obtained in appropriate conditions. The reaction was precisely predicted by the developed mathematical model. Kinetic studies were performed with both free and immobilised enzyme and the later was found to retain approximately 25% of free enzyme activity and had the activity half-life of 9 days.

Keywords L-Malic acid · Microreactor · Fumarase · Immobilisation · Mathematical model

List of Symbols

a	Catalyst activity
c_f	Fumaric acid concentration, mol/m^3 (mM)
$c_{f,0}$	Fumaric acid inlet concentration, mol/m^3 (mM)
c_m	L-Malic acid concentration, mol/m^3 (mM)
$c_{m,0}$	L-Malic acid inlet concentration, mol/m^3 (mM)
D_{AB}	Molecular diffusion coefficient of solute A in solvent B
D_f	Molecular diffusion coefficient of fumaric acid in water, m^2/s
D_m	Molecular diffusion coefficient of L-malic acid in water, m^2/s
H	Microchannel height, m
k_d	Deactivation rate constant, 1/day
$K_{M,f}$	Michaelis constant for fumaric acid, mol/m^3 (mM)
$K_{M,m}$	Michaelis constant for L-malic acid, mol/m^3 (mM)
L	Microchannel length, m
r_1	Rate of fumaric acid hydration, U/L
r_2	Rate of L-malic acid dehydration, U/L
t	Time, s (min)
T	Temperature, °C (K)
V	Volume, m^3 (l, ml)
V_A	Molar volume of the solute, m^3/mol
V_B	Molar volume of solvent (water), m^3/mol
v_{max}	Maximal reaction rate, U/mg
v_ξ	x-Directional velocity of aqueous phase, m/s
W	Microchannel half-width, m
X	Conversion, %
x	Coordinate in the direction of channel length, m
y	Coordinate in the direction of channel width, m
z	Coordinate in the direction of channel height, m

Greek variables

γ	Mass of active enzyme, mg/l
η_B	Solvent (water) dynamic viscosity, kg/m s
ξ	Dimensionless-independent variable, x/W
ψ	Dimensionless-independent variable, y/W
ω	Dimensionless-independent variable, z/W

1 Introduction

Microreactors have many advantages over conventional, larger scale systems, but the risk associated with the introduction of new technologies has prevented them to

G. Stojkovič · I. Plazl · P. Žnidaršič-Plazl (✉)
Faculty of Chemistry and Chemical Technology, University of Ljubljana, Aškerčeva 5, 1000 Ljubljana, Slovenia
e-mail: polona.znidarsic@fkkt.uni-lj.si

enter into production lines in the past. In recent years, however, intensive investigation on possibilities to incorporate microreactor technology in chemical and biochemical processes by industry and academia has shown that microreactor technology is developed enough to present a serious alternative to classical production systems. Although application in industry proceeds in a more cautious way as many factors need to be taken into account (risks, reliability, a need for trained personal, etc.), several companies consider to implement or have already implemented microreactors in their production halls (Roberge et al. 2005; Rouhi 2004; Fernandes 2010). Thereby the majority of a process or only a part of it can be performed using microstructured devices, depending on the suitability and advantages for specific process (Kirschneck and Tekautz 2007). Apart from the reaction steps, downstream processing can be also enhanced by the use of microstructured devices (Žnidaršič-Plazl and Plazl 2007).

Reactions are, whenever possible, performed in continuous flow technique, which has many advantages comparing to batch reactions, among others higher productivity, acceleration of reaction and higher yield (Wiles and Watts 2008). The drawback of continuous processes is lack of flexibility, which is a big problem particularly in fine chemicals and pharmaceutical industry where the production volumes are relatively small. Dedicated continuous systems are therefore often too expensive. On the other hand, batch and semi-batch systems are more economical, as different reactions can be consecutively performed in the same reactor. Unfortunately, the efficiency of batch systems is usually inferior to that achieved in continuous systems. There is therefore a need for highly efficient and versatile systems and microreactors could be the answer to these needs as they have all the advantages of classical continuous systems but also the versatility of batch systems (Roberge et al. 2005).

In addition, microreactors have other advantages over classical systems (batch and continuous), namely high surface to volume ratio, well-defined reaction times, ability to automate the process and numbering-up concept instead of traditional scale-up (Miyazaki and Maeda 2006). As conditions in microreactors can be precisely controlled also the quality of products can be improved. These properties could make microreactors the system of choice for many chemical and biochemical reactions (Wiles and Watts 2008). Furthermore, microreactor technology brings reduction in reactor size class, which allows a new design of production plants that reduces investment capital and energy costs as well as environmental impact by reducing the size of production plants (Pohar and Plazl 2009).

As with classical systems, microreactors can be used with both immobilised and free catalyst. In chemical and biochemical processes, catalyst immobilisation offers some advantages compared to the use of free catalysts, most notably good catalyst–product separation, easy operation, and the possibility of reuse. Also, the stability of biological catalysts (enzymes) can be improved (Pandya et al. 2005). As a consequence, many immobilisation methods have been developed for different materials and catalysts types, including well known biotin–avidin system, 3-aminopropylsilanetriethoxysilane-glutaraldehyde immobilisation and entrapment into hydrogels (Miyazaki and Maeda 2006).

Many research groups have shown that biocatalytic reactions are possible in microchannels and most of them also demonstrated very good results when compared to conventional systems (Thomsen and Nidetzky 2009; Miyazaki and Maeda 2006). For obvious reasons, there is a lack of information regarding development of biocatalytic microsystems from industry. There are some patents granted to descriptions of biochemical processes in microreactors, but these are mainly dealing with the development of Lab-on-a-chip systems which are analytical rather than biotransformation systems (Hessel et al. 2008). However, there were some suggestions that industry, especially pharmaceutical, is considering implementation of microsystems (Roberge et al. 2005; Rouhi 2004). Those could also include biotransformation processes. Taking into account the importance of enzymes for catalysis in classical systems and the trend towards more biologically catalysed reactions for economical as well as environmental reasons, more microbioreactor systems are expected to be implemented into industrial processes (Tišma et al. 2009; Koch et al. 2008).

Continuous microreactor biotransformation system could be the way to a more efficient and economical production of many important compounds, among them organic acids. L-Malic acid (2-hydroxybutanedioic acid) is a major component of different plants and is the second most important acidulent in food industry. It is also used in pharmaceutical industry and medicine (Presečki et al. 2009). Future utilization could also include the use of L-malic acid as a chemical building block, which could in turn increase the needed amount of this compound as high as 200,000 tons per year (Sauer et al. 2008). There is therefore a pronounced need to explore new ways of more efficient L-malic acid production.

L-Malic acid has been industrially produced in several ways. The most widespread is chemical synthesis from maleic or fumaric acid at high temperature and high pressure that yields a DL racemic mixture (Goldberg et al. 2006). On the other hand, stereospecifically pure L-malic acid is produced with different species of immobilised yeast (*Saccharomyces cerevisiae* being dominant since 1990s) in an enzymatic reaction catalysed by fumarase as shown in Fig. 1 (Peleg et al. 1988; Presečki et al. 2007). In this reaction, L-malic acid is synthesized by hydration of

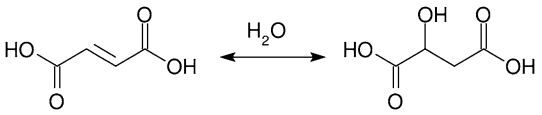

Fig. 1 Conversion of fumaric acid (*left*) to L-malic acid (*right*)

fumaric acid. It is a reversible reaction with equilibrium at approximately 80% of L-malic acid at 30°C (Presečki et al. 2007). L-Malic acid production has also been performed by purified enzymes that were entrapped in hydrogels (Marconi et al. 2001) or immobilised within membrane reactor (Presečki et al. 2009).

Fumarase (EC 4.2.1.2), the enzyme responsible for the biotransformation of fumaric acid, is a tetrameric protein belonging to the group of hydroliases. It has a molecular weight of 194 kDa and consists of four identical subunits linked by noncovalent bonds (Marconi et al. 2001). It is an enzyme of citric acid cycle and is present in mitochondria of eukaryotic cells and cytoplasm of prokaryotic and eukaryotic cells (Sacchettini et al. 1986). Purified fumarase production system has an advantage over whole cell production systems as 10^5 fold higher activity can be observed (Presečki et al. 2009). We supposed that high activity could be well paired with fast mass transfer rate in microreactor system.

The purpose of our research was to set up a continuous system for L-malic acid production from fumaric acid in a glass microreactor using surface-immobilised fumarase that explores the possibilities for microreactor-based biotransformation process. The performance of this reactor was compared to batch reactor and a mathematical model was developed that predicts microreactor performance. In addition, the stability of immobilised fumarase was determined and compared with free enzyme stability.

2 Materials

2.1 Chemicals

3-Aminopropyltriethoxy silane (APTES), fumaric acid, L-malic acid, and glutaraldehyde were from Aldrich (St. Louis, MO, USA). Toluene was from Merck (Darmstadt, Germany). Deionised water was used.

2.2 Enzyme

Fumarase from porcine heart was from Sigma-Aldrich (St. Louis, MO, USA).

2.3 Microreactors

In our experiments, glass microreactors (332 or 664 mm length, 220 μm width, and 100 μm height) from Micronit Microfluidics (B.V., Enschede, The Netherlands) and syringe pumps (PHD 4400 Syringe Pump Series) from Harvard Apparatus (Holliston, USA) were used. Photograph of 332-mm long microreactor with one inlet and outlet is presented in Fig. 2d.

3 Methods

3.1 Immobilisation of fumarase on to microreactor walls

Enzyme immobilisation technique on the microchannel surface is loosely based on the work from Shriver-Lake et al. (2002). Reactors were first cleaned with 4 M NaOH at 90°C and then treated with 5 M HNO_3 for 1 h at 90°C. 10% toluene solution of APTES was then introduced into microchannels for 24 h, followed by 5% glutaraldehyde solution for 4 h. After every treatment, microreactors were thoroughly washed with deionised water. Enzyme in concentration of 0.3 mg/ml was then introduced in the microreactor and left to attach for 18 h at room temperature. After immobilisation, unbound enzyme was washed out with deionised water.

3.2 Biotransformation in microreactors

Reactions were carried out at 30°C with flow rates from 0.5 to 500 μl/min and with different inlet fumaric acid concentrations (from 5 to 500 mM). Fumaric acid was prepared in 0.1 M phosphate buffer (pH 7). Outflow was collected for fumaric acid concentration determination. All reactions were performed at least thrice.

3.3 Reaction kinetics

Batch reactions were carried out at 30°C in 1 ml cuvettes with the final enzyme concentration of 1.45 mg/l. Fumaric acid and L-malic acid prepared in 0.1 M phosphate buffer (pH 7) and with concentrations from 1 to 60 mM were used. Reaction was followed spectrophotometrically at 290 nm. Fumarase activity was determined by initial rates method and kinetic parameters were then calculated by non-linear regression assuming Michaelis–Menten kinetics with product inhibition using QtiPlot software (Copyright by Ion Vasilief). Experiments were carried out in at least five replicates.

3.4 Determination of fumaric and L-malic acid concentration

Reactions in batch system were followed spectrophotometrically and the concentration of fumaric acid was

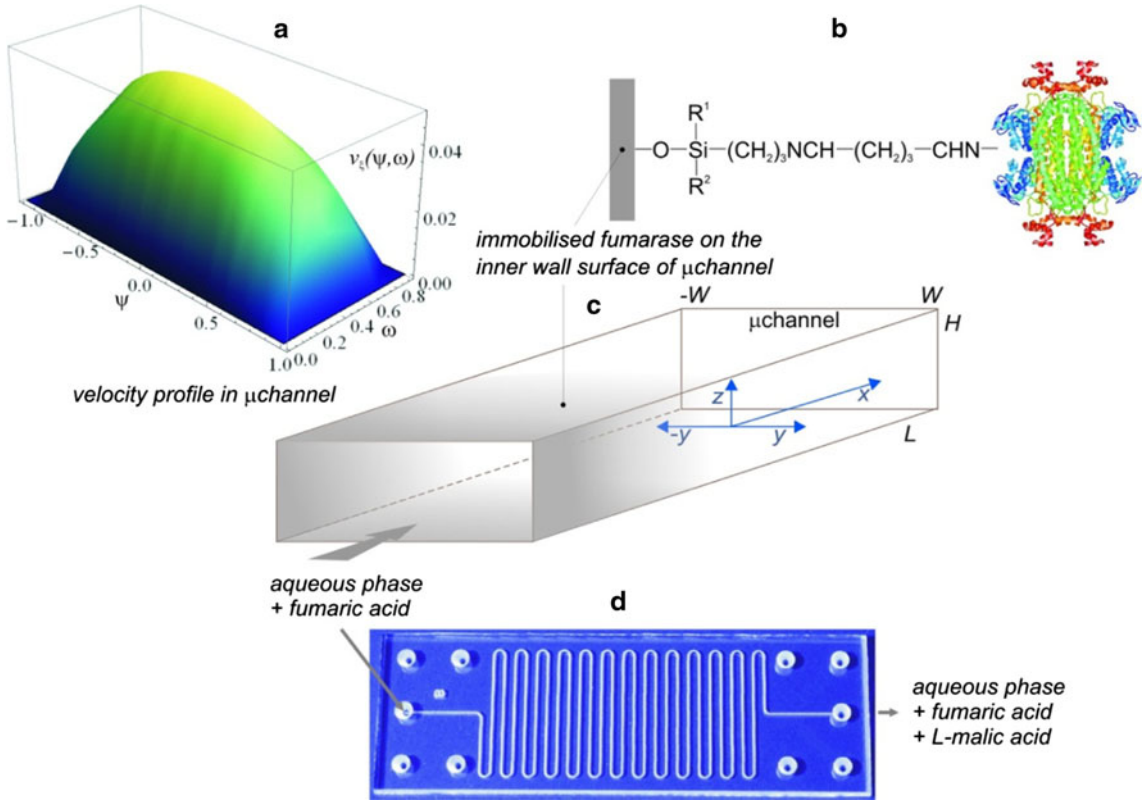

Fig. 2 Presentation of the microreactor system used: **a** velocity profile in a microchannel, **b** a scheme of enzyme immobilisation principle, **c** scheme of a microchannel and **d** a microreactor picture

determined at 290 nm (Cary 50, Varian Australia Pty Ltd, Mulgrave, Australia). L-Malic acid concentration was then calculated from fumaric acid concentration. Prior to spectrophotometrical measurements, samples were diluted as needed with phosphate buffer.

3.5 Determination of enzyme stability

In order to determine enzyme catalytic stability, enzymes were immobilised into microreactors as described above. Conversion of fumaric to L-malic acid was started with 100 mM fumaric acid as substrate at a flow rate of 2 μl/min. Samples were collected daily and the concentration of fumaric acid was measured as described. Conversions were then calculated and compared to initial conversion and ratios were plotted against time. The experiments were performed in triplicates.

3.6 Immobilised enzyme quantification

Once enzymes were immobilised and the activity measured, enzymes were detached from the microreactor surface using 0.1 M HCl. The effluent from the reactor was collected in a microcentrifuge tube and the protein concentration measured spectrophotometrically at 280 nm using Nanodrop ND1000 (Thermo Fischer Scientific, Waltham, MA, USA). The experiments were performed in six replicates.

3.7 Estimation of protein diameter and microchannel surface load

To estimate fumarase diameter and microchannel surface load, fumarase mass was first calculated from molar mass of the enzyme ($M = 200{,}000$ g/mol). Assuming a spherical shape of molecules and a density of $\rho = 1.41$ g/ml (Fischer et al. 2004), the molecule diameter was then calculated.

Number of enzymes per area unit was estimated supposing total coverage of the microreactor wall surface in one layer. Theoretical enzyme load was thereof calculated.

4 Mathematical model

A theoretical description of the reaction–diffusion processes of homogeneous enzyme reaction in a microreactor was presented considering the velocity profile for laminar flow of aqueous phase at steady-state conditions. A 3D mathematical model in dimensionless form, containing convection, diffusion, and reversible reaction term was

developed to analyse and to forecast the microreactor performance. Scheme of the microchannel with immobilised fumarase (Fig. 2b) on the inner wall surface is presented in Fig. 2c.

In order to simulate L-malic acid production within a microreactor with surface immobilised fumarase, the velocity profile was first setup. Therefore, the Poiseuille-type flow was developed considering steady state flow of aqueous phase and neglecting compressibility and the gravitational force (Tišma et al. 2009). The 3D graphical visualization of a fully developed flow pattern in a microchannel is presented in Fig. 2a.

Dimensionless partial differential equations for steady-state conditions in the single pass microreactor system with the associated boundary conditions are:

- for fumaric acid, c_f

$$v_\xi(\psi,\omega)\frac{\partial c_f}{\partial \xi} = \frac{D_f}{W}\left(\frac{\partial^2 c_f}{\partial \xi^2}+\frac{\partial^2 c_f}{\partial \psi^2}+\frac{\partial^2 c_f}{\partial \omega^2}\right) \tag{1}$$

with the associated boundary conditions:

$$\begin{aligned}
&c_f(0,\psi,\omega) = c_{f,0}, \quad -1\le\psi\le 1, \quad 0\le\omega\le\frac{H}{W};\\
&\frac{\partial c_f\left(\frac{L}{W},\psi,\omega\right)}{\partial\xi} = 0, \quad -1\le\psi\le 1, \quad 0\le\omega\le\frac{H}{W};\\
&\frac{\partial c_f(\xi,\pm 1,\omega)}{\partial\psi} = (r_1-r_2)\frac{\Delta\psi W}{D_f}, \quad 0<\xi<\frac{L}{W}, \quad 0\le\omega\le\frac{H}{W};\\
&\frac{\partial c_f(\xi,\psi,0)}{\partial\omega} = (r_1-r_2)\frac{\Delta\omega W}{D_f}, \quad 0<\xi<\frac{L}{W}, \quad -1<\psi<1;\\
&\frac{\partial c_f\left(\xi,\psi,\frac{H}{W}\right)}{\partial\omega} = (r_1-r_2)\frac{\Delta\omega W}{D_f}, \quad 0<\xi<\frac{L}{W}, \quad -1<\psi<1;
\end{aligned} \tag{2}$$

for L-malic acid, c_m

$$v_\xi(\psi,\omega)\frac{\partial c_m}{\partial \xi} = \frac{D_m}{W}\left(\frac{\partial^2 c_m}{\partial \xi^2}+\frac{\partial^2 c_m}{\partial \psi^2}+\frac{\partial^2 c_m}{\partial \omega^2}\right) \tag{3}$$

with the associated boundary conditions:

$$\begin{aligned}
&c_m(0,\psi,\omega) = 0, \quad -1\le\psi\le 1, \quad 0\le\omega\le\frac{H}{W};\\
&\frac{\partial c_m\left(\frac{L}{W},\psi,\omega\right)}{\partial\xi} = 0, \quad -1\le\psi\le 1, \quad 0\le\omega\le\frac{H}{W};\\
&\frac{\partial c_m(\xi,\pm 1,\omega)}{\partial\psi} = (r_2-r_1)\frac{\Delta\psi W}{D_m}, \quad 0<\xi<\frac{L}{W}, \quad 0\le\omega\le\frac{H}{W};\\
&\frac{\partial c_m(\xi,\psi,0)}{\partial\omega} = (r_2-r_1)\frac{\Delta\omega W}{D_m}, \quad 0<\xi<\frac{L}{W}, \quad -1<\psi<1;\\
&\frac{\partial c_m\left(\xi,\psi,\frac{H}{W}\right)}{\partial\omega} = (r_2-r_1)\frac{\Delta\omega W}{D_m}, \quad 0<\xi<\frac{L}{W}, \quad -1<\psi<1;
\end{aligned} \tag{4}$$

The definition of boundary conditions is based on the diffusional mass transport of fumaric acid to and L-malic acid from microreactor walls, where enzymatic reaction takes place. As noted in the literature (Presečki et al. 2007), fumaric acid hydratation (r_1) and L-malic acid dehydration (r_2) is well described with Michaelis–Menten kinetics with competitive product inhibition:

$$r_1 = \frac{v_{\max,1}\cdot\gamma\cdot a_f}{K_{M,f}\left(1+\frac{c_m}{K_{i,m}}\right)+c_f}; \quad r_2 = \frac{v_{\max,2}\cdot\gamma\cdot a\cdot c_m}{K_{M,m}\left(1+\frac{c_f}{K_{i,f}}\right)+c_m}. \tag{5}$$

To describe the deactivation process observed in experimental studies, the activity term a was added to the reaction rate equations which can be described by an nth order equation (Levenspiel 1999):

$$-\frac{da}{dt} = k_d a^n \tag{6}$$

4.1 Estimation of diffusion coefficients

Molecular diffusion coefficients of fumaric and L-malic acid in water were calculated using Scheibel empirical correlation (Li and Carr 1997):

$$D_{AB} = \frac{8.2\cdot 10^{-8} T}{\eta_B\cdot \overline{V}_A^{1/3}}\left[1+\left(\frac{3\cdot\overline{V}_B}{\overline{V}_A}\right)\right]^{2/3} \tag{7}$$

4.2 Numerical solution

Finite differences on the 3D Cartesian grid were used to replace the partial derivatives in the presented model equations. In order to solve the complex nonlinear system of model equations, MATLAB environment was used to develop the code, which enabled fast converging to the equations solutions.

5 Results and discussion

5.1 Enzyme immobilisation and stability

In our experiments, surface immobilised fumarase was used to take full advantage of an increased surface-to-volume ratio of microreactors. Prior to immobilisation, microchannels were cleaned with NaOH and then treated with 5 M nitric acid at 90°C to introduce hydroxyl groups on the surface. Then APTES was used to introduce NH_2 groups on the surface. Finally, fumarase was covalently immobilised to the microreactor surface according to Shriver-Lake et al. (2002) with glutaraldehyde as a linker between surface and enzyme bound NH_2 groups as shown in Fig. 2b. In order to assess immobilisation efficiency, protein concentration was estimated after washing the enzyme out from the microchannel. Approximately 2.2 μg of fumarase was measured in the chosen microchannel

which corresponds to 0.61 μg fumarase per cm^2 of microreactor wall surface and 300 μg of enzyme per ml. This would therefore mean approximately 70% immobilisation efficiency in respect to maximal theoretical enzyme load, estimated from protein size as described under Sect. 3, which was calculated to be 3.1 μg for this microreactor. In theoretical load calculation it was assumed that the enzyme has a spherical shape, a density of 1.41 g/ml and that it covers the entire available surface of the microchannel walls. The later assumption could not be valid as enzymes do not adapt their shape to fit a space and can therefore not be packed as densely. Immobilisation efficiency was therefore higher than calculated, presumably close to 100%. To increase enzyme load even more, the use of nanostructured surface of the channels (Thomsen and Nidetzky 2009) or sol–gel technique were suggested.

Immobilised fumarase activity was followed for a prolonged period of time to determine operational stability and the results are shown in Fig. 3. Modelling of the observed deactivation was approached by applying the reaction kinetics with an activity term (Eqs. 5 and 6) to the dynamic model. Based on the experimental data, the kinetics of the deactivation process could be best described as a second-order reaction ($n = 2$ in Eq. 6):

$$\alpha = \frac{1}{k_d \cdot t + 1}. \tag{8}$$

and deactivation rate constant, k_d, evaluated by the best-fit method, was calculated to be 0.31 per day.

Based on fumarase kinetics, described by Michaelis–Menten equation with competitive product inhibition (Eq. 5), the apparent activity half-life, at which the conversion becomes half of the initial one, was calculated to be approximately 9 days, which is in accordance with experimental data (Fig. 3). These results are in agreement with previously published data for covalently bound fumarase (Marconi et al. 2001). Loss of activity is probably the result of enzyme denaturation.

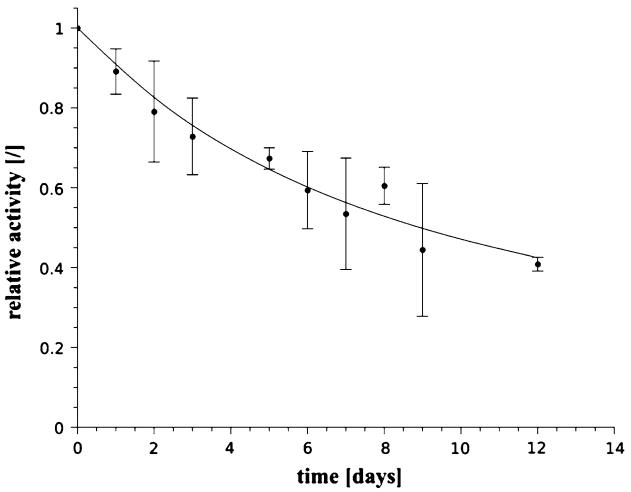

Fig. 3 Enzyme activity as a function of time. Mean experimental data (*points*) with standard deviations (*brackets*) are given together with model predictions (Eqs. 1–8; *line*); ($c_{f,0} = 100$ mM, flow rate of fumaric acid = 2 μl/min)

5.2 Biotransformations with fumarase

In order to be able to compare batch and continuous microreactor performance, fumarase was first tested in a batch system at various substrate and product concentrations. Results, presented in Fig. 4, showed a very good correlation with Michaelis–Menten kinetic model with competitive product inhibition (Eq. 5), known to describe fumarase behaviour (Presečki et al. 2007). The associated kinetic parameters determined are shown in Table 1.

Performance of immobilised fumarase microreactor was then tested at various substrate concentrations and flow rates and the activity of free and immobilised enzyme was compared. Immobilised enzyme was found to retain approximately 25% of activity of the free enzyme, which is considerably better than reported in the literature for covalently immobilised enzyme (10%) but less than for entrapped enzyme (40%) (Marconi et al. 2001). Activity drop can be due to wrong enzyme orientation on the surface resulting in active site being inaccessible to the substrate or decreased activity through structural changes imposed by the microchannel surface.

A comparison of experimental data with model predictions for freshly immobilised enzyme is shown in Fig. 5a. It can be seen that mathematical model precisely predicted microreactor performance and that under appropriate conditions, i.e. with longer retention times (8–15 min), conversion of fumaric to L-malic acid effectively reached equilibrium at approximately 80%, which is in accordance with previously published data for free fumarase (Presečki et al. 2009). When lower substrate concentrations were used, 80% conversion could be achieved at adequately shorter retention times.

Regarding our previous observations that immobilised enzyme retained 25% of activity of the free enzyme, 25% of total enzyme was assumed as active enzyme concentration in the developed model ($0.25 \cdot \gamma$ in Eq. 5), while the kinetic parameters of free enzyme were supposed to be retained in immobilised form. Even though the immobilised enzyme molecules are usually only partially active and/or accessible for the substrate and therefore have altered v_{max}, K_m, and K_i values, the model precisely predicted system performance at various operating conditions as shown in Fig. 5a. Furthermore, concentration profiles of a particular component within the microchannel were obtained by a numerical solution of the nonlinear system of partial differential equations based on the previously

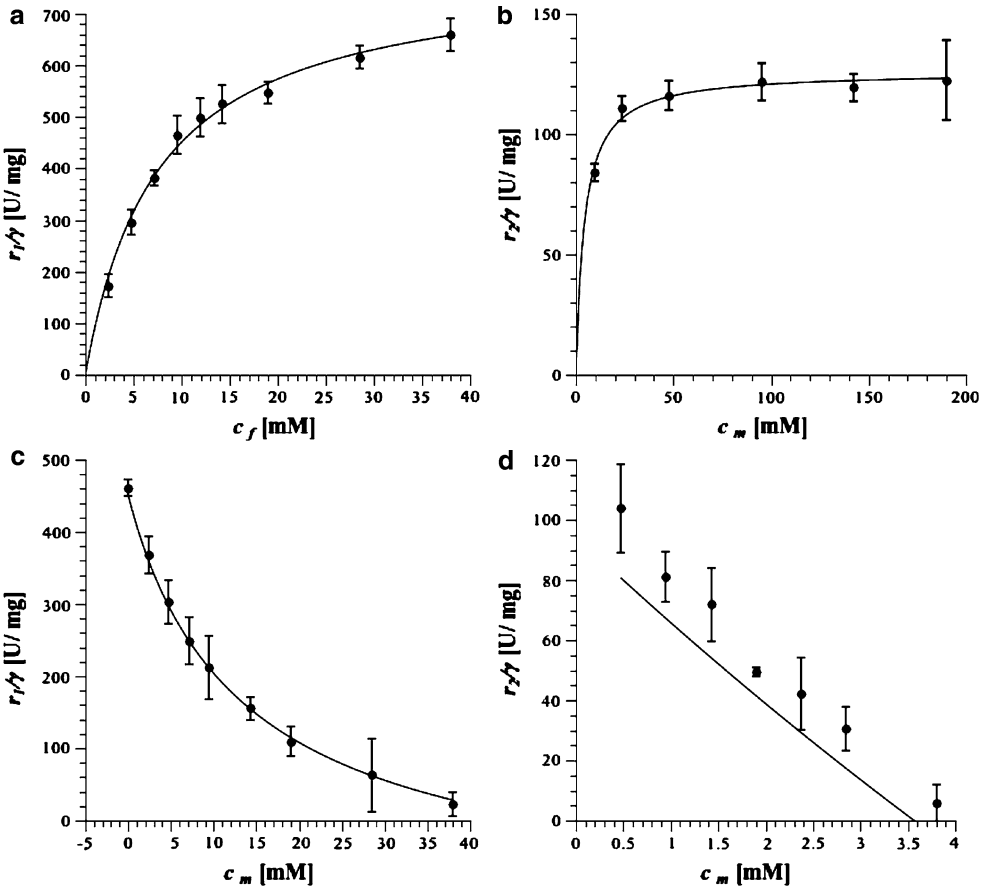

Fig. 4 Kinetics of free fumarase in a batch system (30°C, 100 mM phosphate buffer, $\gamma = 1.45$ mg/l): **a** specific rate of fumaric acid hydration, defined per catalyst amount (r_1/γ) at increasing c_f; **b** specific rate of L-malic acid dehydration (r_2/γ) at increasing c_m; **c** specific rate of fumaric acid hydration (r_1/γ) at $c_{f,0} = 9.5$ mM and at increasing c_m; **d** specific rate of L-malic acid dehydration (r_2/γ) at $c_{m,0} = 19$ mM and at increasing c_f. *Points* indicate experimental data, *brackets* the standard deviations and *lines* represent model predictions

Table 1 Kinetic parameters of free porcine heart fumarase as determined from batch experiments

Fumaric acid hydration	
$v_{max,\ 1}$ (U/mg)	788 ± 21
$K_{M,f}$ (mM)	7.46 ± 0.58
$K_{i,f}$ (mM)	6.97 ± 0.14
D_f (cm^2/s)	1.07×10^{-5}
L-Malic acid dehydration	
$v_{max,\ 2}$ (U/mg)	126 ± 1.9
$K_{M,m}$ (mM)	6.65 ± 0.54
$K_{i,m}$ (mM)	9.76 ± 1.2
D_m (cm^2/s)	1.06×10^{-5}

described velocity profile and kinetic model with inhibition by both substrates (Eqs. 1–5). As expected, results of numerical simulation of substrate and product concentration profile at 5 mM inlet concentration of fumaric acid and flow rate of 50 µl/min revealed the largest fumaric acid concentration drop and L-malic acid concentration rise at the surface area, where enzyme reaction takes place (Fig. 5b, c).

The calculated volumetric productivity at the highest tested fumaric acid inlet concentration of 50 mM was 2.57 mM/min at residence time 14.6 min, where also almost 80% conversion was achieved. This is more than three times higher than reported for continuous L-malic acid production within enzyme membrane reactor, where the highest volumetric productivity of 0.81 mM/min was achieved at residence time of 53 min and where the conversion was only 68% (Presečki et al. 2009). These results again confirm process intensification at the microreactor scale.

It must, however, be noted that volumetric productivity and conversion values presented in Fig. 5 are only valid with freshly immobilised enzymes. Due to the observed enzyme deactivation, the drop of volumetric productivity and conversion with process time is inevitable. Enzyme stability should therefore be improved, either by means of enzyme entrapment or by multipoint covalent immobilisation coupled with additional crosslinking (Marconi et al. 2001; Mateo et al. 2007), which could lead to a prolonged enzyme half-life, more suitable for production systems.

6 Conclusions

A continuous system for L-malic acid production in a microreactor was developed that is based upon a simple and efficient method for fumarase immobilisation. The

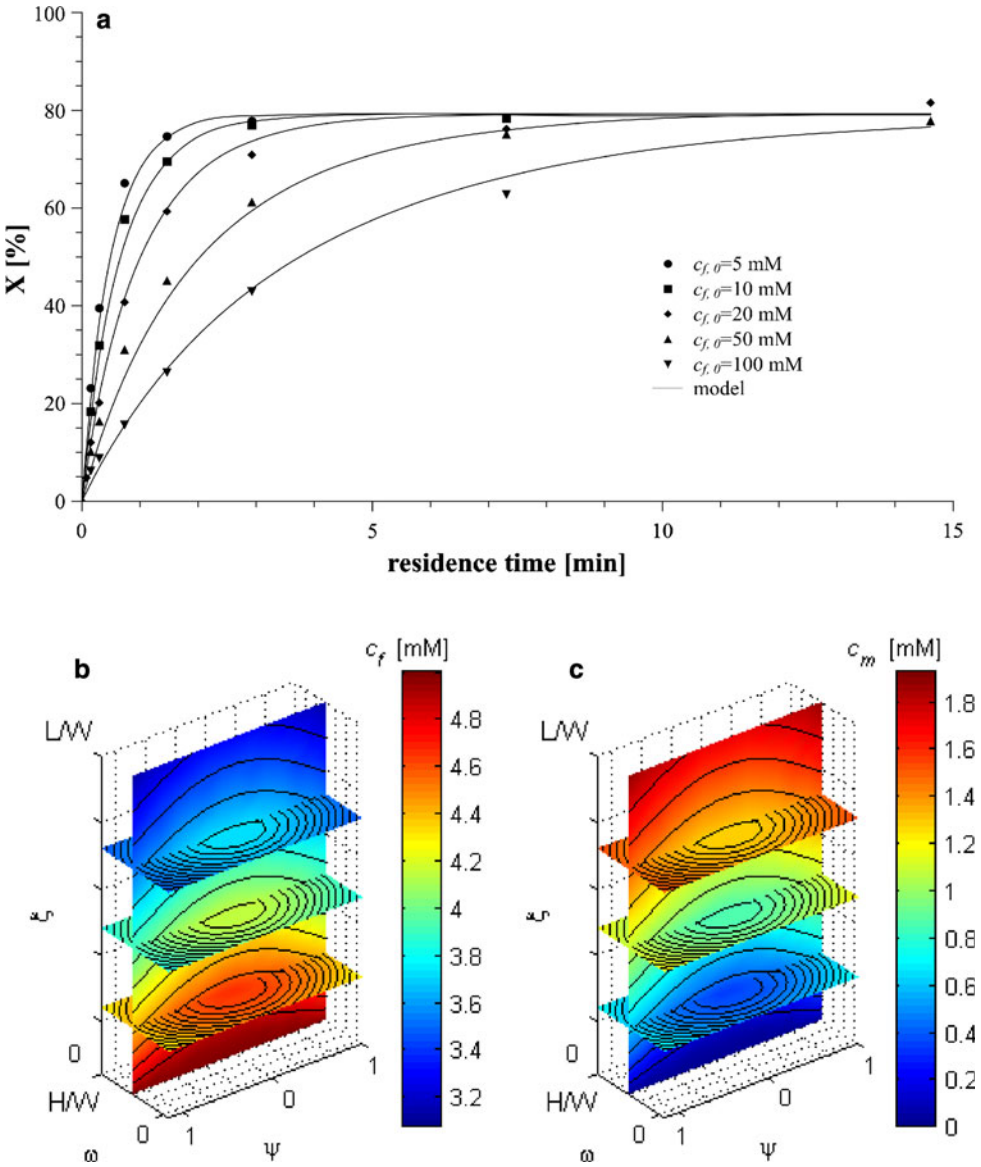

Fig. 5 Comparison of model predictions with experimental data. **a** Conversion of fumaric acid to L-malic acid as a function of residence time and inlet fumaric acid concentration. In all experiments, freshly immobilised enzymes were used. *Points* represent experimental data and *curves* represent model predictions. Mathematical simulations of concentration profile within the microchannel for fumaric acid hydration at 5 mM inlet concentration of fumaric acid and at flow rate of 50 µl/min: **b** fumaric acid depletion and **c** L-malic acid synthesis

enzyme retains approximately 25% of the free enzyme activity, which is better than reported in literature. In future work, enzyme stability should be addressed as activity half-life was found to be 9 days. The mathematical model developed enables description and optimization of the process. Overall, we found the described approach to be suitable for intensification of L-malic acid production.

The process could be further enhanced by integrating a method for L-malic acid separation from fumaric acid, possibly by a consecutive reactor with immobilised aspartase which converts the remaining fumaric acid to aspartic acid which can be efficiently separated from L-malic acid (Chen et al. 1994).

Acknowledgments This work was financially supported through Grant P2-0191, and G. Stojkovič was supported through PhD Grant 1000-08-310200, both provided by the Ministry of Higher Education, Science and Technology of the Republic of Slovenia. Measurements of protein concentrations were performed with kind help from Mojca Benčina, PhD (National Institute of Chemistry, Slovenia). We are also grateful to Andrej Pohar (Faculty of Chemistry and Chemical Technology, University of Ljubljana, Slovenia) for his help with mathematical data manipulation and presentation.

References

Chen ST, Duh SC, Wang KT (1994) Facile synthesis of L-malic acid by a consecutive enzymatic reaction. Biotechnol Lett 16:355–358

Fernandes P (2010) Minituarization in biocatalysis. Int J Mol Sci 11:858–879

Fischer H, Polikarpov I, Craievich AF (2004) Average protein density is a molecular-weight-dependent function. Protein Sci 13:2825–2828

Goldberg I, Stefan Rokem J, Pines O (2006) Organic acids: old metabolites, new themes. J Chem Technol Biotechnol 81:1601–1611

Hessel V, Knobloch C, Löwe H (2008) Review on patents in microreactor and micro process engineering. Recent Pat Chem Eng 1:1–16

Kirschneck D, Tekautz G (2007) Integration of a Microreactor in an Existing Production Plant. Chem Eng Technol 30:305–308

Koch K, van den Berg RJF, Nieuwland PJ, Wijtmans R, Wubbolts MG, Schoemaker HE, Rutjes FPJT, van Hest JCM (2008) Enzymatic synthesis of optically pure cyanohydrins in microchannels using a crude cell lysate. Chem Eng J 135:89–92

Levenspiel O (1999) Chemical reaction engineering, 3rd edn. Wiley, New York

Li J, Carr PW (1997) Accuracy of empirical correlations for estimating diffusion coefficients in aqueous organic mixtures. Anal Chem 69:2530–2536

Marconi W, Faiola F, Piozzi A (2001) Catalytic activity of immobilized fumarase. J Mol Catal B 15:93–99

Mateo C, Palomo JM, Fernandez-Lorente G, Guisan JM, Fernandez-Lafuente R (2007) Improvement of enzyme activity, stability and selectivity via immobilization techniques. Enzyme Microb Technol 40:1451–1463

Miyazaki M, Maeda H (2006) Microchannel enzyme reactors and their applications for processing. Trends Biotechnol 24:463–470

Pandya PH, Jasra RV, Newalkar BL, Bhatt PN (2005) Studies on the activity and stability of immobilized α-amylase in ordered mesoporous silicas. Micropor Mesopor Mater 77:67–77

Peleg Y, Stieglitz B, Goldberg I (1988) Malic acid accumulation by Aspergillus flavus. Appl Microbiol Biotechnol 28:69–75

Pohar A, Plazl I (2009) Process intensification through microreactor application. Chem Biochem Eng Q 23:537–544

Presečki AV, Zelić B, Vasić-Rački Đ (2007) Comparison of the L-malic acid production by isolated fumarase and fumarase in permeabilized baker's yeast cells. Enzyme Microb Technol 41:605–612

Presečki AV, Zelić B, Vasić-Rački Đ (2009) Modelling of continuous L-malic acid production by porcine heart fumarase and fumarase in yeast cells. Chem Biochem Eng Q 23:519–525

Roberge DM, Ducry L, Bieler N, Cretton P, Zimmermann B (2005) Microreactor technology: a revolution for the fine chemical and pharmaceutical industries? Chem Eng Technol 28:318–323

Rouhi AM (2004) Microreactors eyed for industrial use: hands-on experience with microreactors convinces Sigma-Aldrich of their utility. Chem Eng News. June 29, 2004. Accessed 9 July 2010

Sacchettini JC, Meininger T, Roderick S, Banaszak LJ (1986) Purification, crystallization, and preliminary X-ray data for porcine fumarase. J Biol Chem 261:15183–15185

Sauer M, Porro D, Mattanovich D, Branduardi P (2008) Microbial production of organic acids: expanding the markets. Trends Biotechnol 26:100–108

Shriver-Lake LC, Bryce Gammeter W, Bang SS, Pazirandeh M (2002) Covalent binding of genetically engineered microorganisms to porous glass beads. Anal Chim Acta 470:71–78

Thomsen MS, Nidetzky B (2009) Coated-wall microreactor for continuous biocatalytic transformations using immobilized enzymes. Biotechnol J 4:98–107

Tišma M, Zelić B, Vasić-Rački Đ, Žnidaršič-Plazl P, Plazl I (2009) Modelling of laccase-catalyzed L-DOPA oxidation in a microreactor. Chem Eng J 149:383–388

Wiles C, Watts P (2008) Continuous flow reactors, a tool for the modern synthetic chemist. Eur J Org Chem 1655–1671

Žnidaršič-Plazl P, Plazl I (2007) Steroid extraction in a microchannel system—mathematical modeling and experiments. Lab Chip 7:883–889